

# A UV-responsive Mechanically Robust Insulating Material Achieving Intrinsic Self-Healing of Electrical Tree Damage Based on Reversible Anthracene Photodimerization

*Potao Sun, Zeyan Shi, Wenxia Sima\*, Xinyu Tang, Tao Yuan, Ming Yang, Hang Xu, Zhaoping Li.*

*State Key Laboratory of Power Transmission Equipment Technology, School of Electrical  
Engineering, Chongqing University, Chongqing, 400044, People's Republic of China.*

## 1. Infrared spectroscopy of 9-AMA

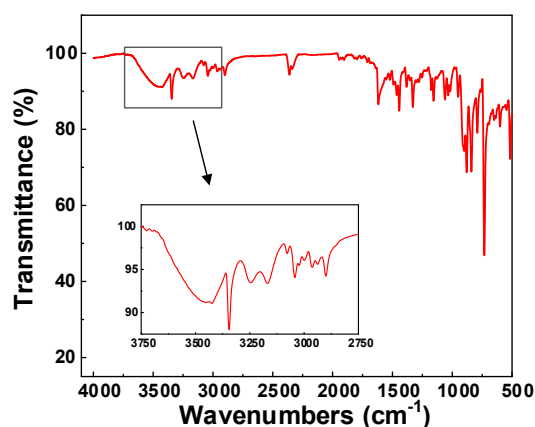


Fig. S1 FTIR spectrum of 9-AMA.

## 2. Curing reaction of epoxy

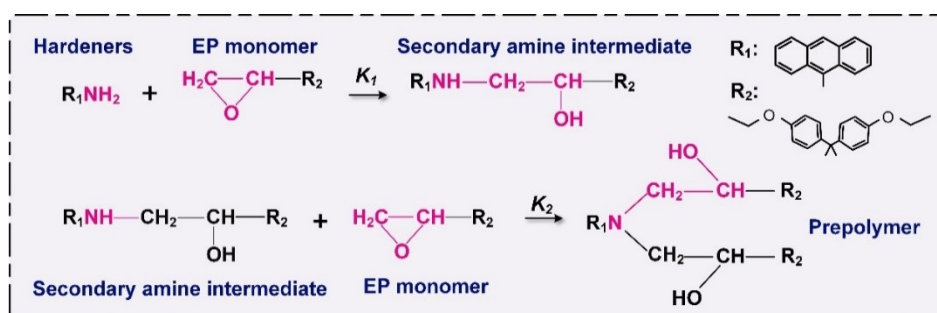


Fig. S2 The curing reaction process of an amine-based curing agent and epoxy group.

## 3.

Table S1. Wechsler hardness and T<sub>g</sub> of ISEP-RAP.

	Shore hardness (HD)	T <sub>g</sub> (°C)
HCIS-EP	81.1	147.5
LCIS-EPP	59.4	82.5

## 4. Method of tensile test

The samples production was referred to the Chinese national standards GB/T 581. As the Fig. S3 (a)-(b) shown, the sample was dumbbell shaped with the thickness of 2mm. The length and width of testing area were 10mm, 4mm respectively. The stretching test of the sample was referred to GB/T 1040.1. Specifically, the sample was placed in the fixture of the tester so that the long axis of the sample was aligned with the axis of the tester. The clamps were adjusted to clamp the sample smoothly and firmly to prevent sample slipping and movement of the clamps during the test, and to avoid clamping forces that might cause cracking or extrusion of the sample. During the test, the sample was

stretched along the longitudinal main axis at the constant speed of 5mm/min until the sample broken or the stress reached the predetermined value of 100N. The load and elongation of the test during this process were measured and recorded. The testing was processed under a testing temperature of  $23 \pm 2$  °C. The model of tensile strength tester was ETM203B (Shenzhen Wance Technologies Co., Ltd, China), which met GB/T16825.1-2008 and GB/T12160-200. The **Fig. S3 (c)-(d)** shows the tester and the fractured sample.

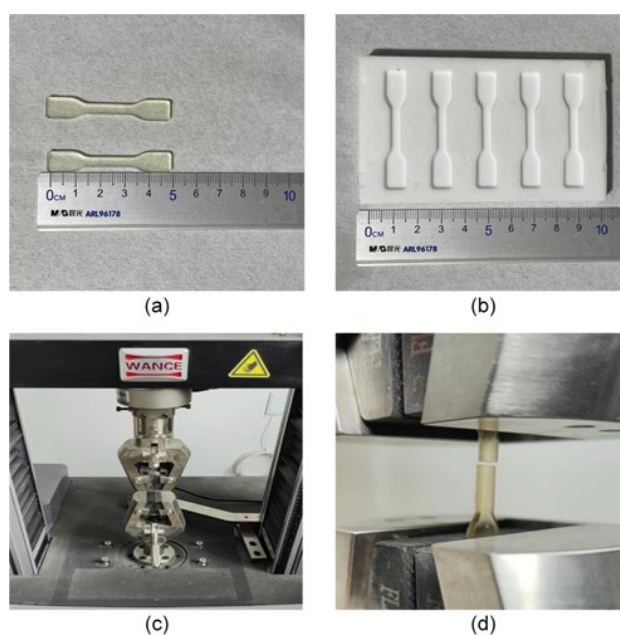
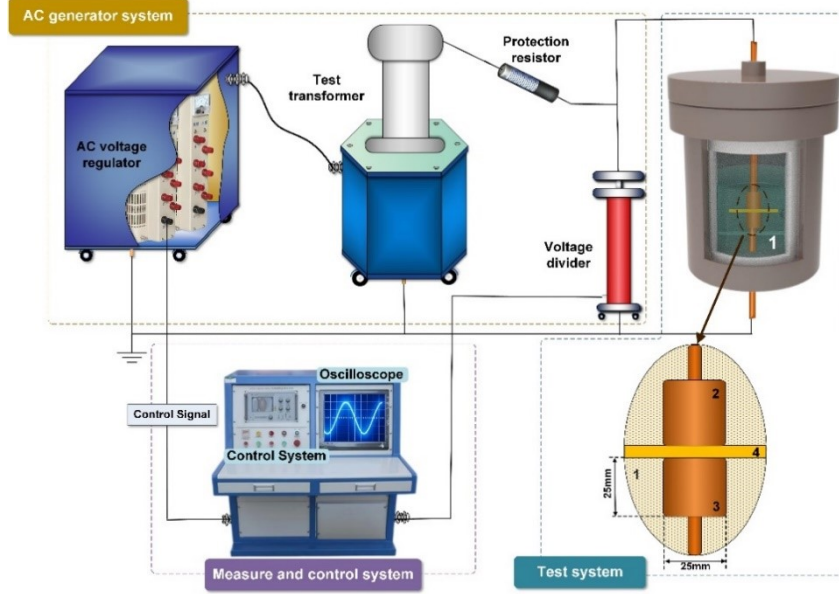


**Fig. S3** (a) samples to be tested, (b) mold of tensile samples, (c) the tensile strength tester and (d) sample that has been stretched to fractured.

## 5. AC breakdown field strength test experimental platform

The AC breakdown field strength of ISEP-RAP is measured by an AC breakdown experimental platform (as shown in **Fig. S4**). The sample to be measured is sandwiched between two cylindrical copper electrodes. The voltage regulator is used to increase the 50Hz power frequency AC voltage under room temperature conditions applied to both ends of the copper electrode at a rate of 0.5kV/s until the material breaks. At this time, the high-voltage power source automatically breaks off, and the monitoring system records the breakdown voltage. After a ten-minute interval, replace the sample with a new one and repeat the above experiment at least 9 times.



1. insulation oil, 2. high voltage electrode, 3. ground electrode, 4. test sample

Fig. S4. Schematic diagram of the AC breakdown test platform.

## 6. Weibull distribution

The probability density function of the Weibull distribution is

$$f(x, \lambda, k) = \begin{cases} \frac{k}{\lambda} \left(\frac{x}{\lambda}\right)^{k-1} e^{-(x/\lambda)^k}, & x \geq 0 \\ 0, & x < 0 \end{cases} \quad (1)$$

Therefore, the cumulative distribution function of the Weibull distribution is

$$F(x, \lambda, k) = 1 - e^{-(x/\lambda)^k} \quad (2)$$

where  $x$  is the electric field strength,  $F$  is the breakdown probability under this field strength,  $k$  shape parameter. When  $k < 1$ , indicating that the probability decreases with the increase of  $x$ ; when  $k = 1$ , indicating that the probability is constant, at this time the Weibull distribution is simplified to an exponential distribution; when  $k > 1$ , the probability increases with the increase of  $x$ , the distribution function is convex and then concave, and the inflection point is:  $(e^{1/k} - 1) / e^{1/k}$ .  $\lambda$  is the scale parameter of the distribution, representing the value of the field strength  $x$  at a failure probability of 63.2%, which is often regarded as the characteristic breakdown field strength of the sample.

The fit of the Weibull distribution to the data can be visually evaluated using a Weibull plot, which is a plot of the empirical cumulative distribution function.  $\mathbf{F}(x)$  is the data on a special axis in the

quantile-quantile plot, The coordinates are  $\ln(-\ln(1-F(x)))$  and  $\ln x$  respectively, which linearizes the cumulative distribution function by this transformation:

$$\begin{aligned} F(x) &= 1 - e^{-(x/\lambda)^k} \\ -\ln(1 - F(x)) &= (x/\lambda)^k \\ \ln(-\ln(1 - F(x))) &= k \ln x - k \ln \lambda \end{aligned} \quad (3)$$

The breakdown field strength data obtained by AC breakdown experiment are numbered from small to large as 1~n, and the empirical distribution function is obtained from n experimental data:  $\hat{F} = \frac{i-0.3}{n+0.4}$ , where i is the rank of this experimental data, n is the total number of experimental data, and p is the failure probability of this experimental data.

### 7. Relative permittivity:

The permittivity is used to indicate the ability of the material to hold the charges. The lower permittivity means the less charge accumulation, which can inhibit electric field distortion, reduce partial discharge or local heating, and provide a more stable insulation environment for the operation of power equipment.

In the polymer dielectric, the permittivity is mainly affected by electron shift polarization and steering polarization. The establishment speed of electron shift polarization is extremely fast within 10<sup>-15</sup>~10<sup>-16</sup>s. The steering polarization takes a longer establishment time within 10<sup>-6</sup>~10<sup>-2</sup>s due to molecular disorder thermal motion, the effect of electric field ordering and the influence of intermolecular forces. Furthermore, with the increase of frequency, the steering polarization is too late to proceed, and only the electron displacement polarization can keep up with the change of the electric field. Therefore, the permittivity of the dielectric under the high-frequency electric field only exists as a major form of electron polarization, which reduces permittivity.

The relative permittivity of the polymer dielectric can be qualitatively analyzed by the Clausius-Mossotti equation formula (4), where  $\epsilon_r$  is the macroscopic relative permittivity of the material,  $\epsilon_0$  is

the vacuum permittivity,  $\alpha$  is the microscopic polarizability, and N is the number of polarized particles per unit volume of the dielectric.

$$\frac{\varepsilon_r - 1}{\varepsilon_r + 2} = \frac{N\alpha}{3\varepsilon_0} \quad (4)$$

Due to the introduction of non-polar and large spatial molecular volume anthracene-dime groups in the molecular network structure, the HCIS-EP reduces the macroscopic relative permittivity of the material and the number of polarized particles per unit volume of the dielectric, resulting in a decrease in the permittivity. The molecular chain in the LCIS-EPP is interrupted due to the cleavage of the anthracene group, the turning polarization is more likely to occur and the relaxation polarization increases, so that the macroscopic permittivity of the material increases significantly, and the anthracene group polymerized into the anthracene group after 365nm treatment, the density of crosslinking is improved, and the high crosslinking state is regenerated, which has the low permittivity brought by the introduction of anthracene groups.

## **8. Electric tree aging experiment**

Using the needle-plate electrode aging experimental platform shown in **Fig. S5** to induce electric branch damage, the sample is placed between the needle plate electrodes to ensure that it was completely wrapped around the needle electrode. The needle plate electrode spacing was 2mm, and its tip radius was 50 $\mu$ m, which can simulate the electrical damage caused by excessive local field strength and charge injection caused by insulation defects in electrical insulation polymer. The sample is immersed in insulating oil to prevent flashover along the surface. By controlling the voltage regulator to apply a 50Hz power frequency voltage from 0kV. When the start-tree voltage is measured, the voltage rise rate is 0.2kV/s, and when an electric tree begins to appear at the needle electrode, the value displayed at this time is recorded as the starting voltage. When the electric tree aging is induced, the voltage rise rate is 2kV/s. While the electric tree is observed for the first time, the voltage is

immediately adjusted to 80% of the voltage at this time, so that the electric tree develops to a length of 600-800  $\mu\text{m}$ , then the voltage at both electrode is removed. The induction of the electric tree damage is finished. The development process of electric tree is shown in **Fig. S6** and video **Movie S1**, and the typical morphologies of electric tree are shown in **Fig. S7**.

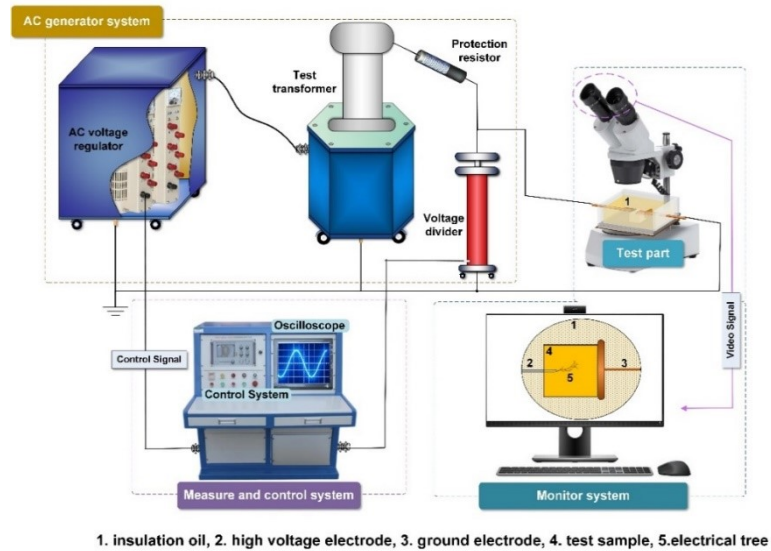


**Fig. S5.** Electric tree aging and online observation platform.

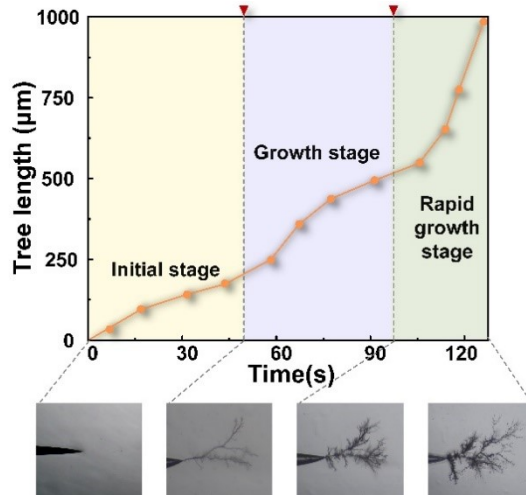


**Fig. S6.** The development process of electric tree.

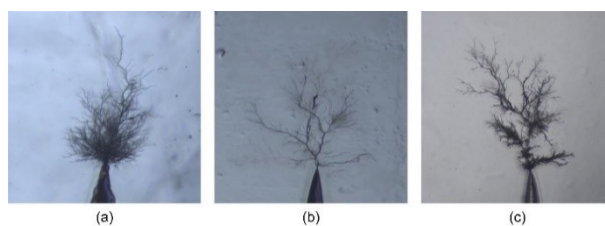


**Fig. S7.** Different types of electric trees: (a) Clumped electric tree, (b) Dendritic electric tree, (c) Composite electric tree.

## 9. Process of healing mechanical scratch

Please see **Movie S2** for details

## 10. Process of healing electric tree damage

Please see **Movie S3** for details

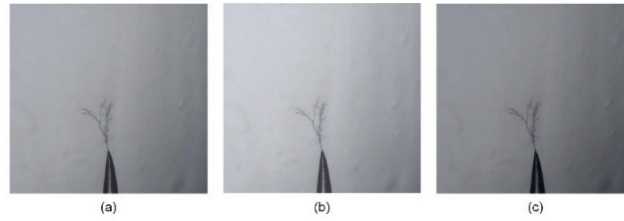


**Fig. S8.** Standard EP with electric tree damage is heated at 80 °C for (a)0min, (b)60min, (c)120min.